Gynecologic Oncology 153 (2019) 405–415

Contents lists available at ScienceDirect

Gynecologic Oncology

journal homepage: www.elsevier.com/locate/ygyno

Inhibition of fascin in cancer and stromal cells blocks ovarian cancer metastasis

Sean McGuire [a], Betul Kara [a], Peter C. Hart [a], Anthony Montag [b], Kristen Wroblewski [c], Sarah Fazal [d], Xin-Yun Huang [e], Ernst Lengyel [a,*], Hilary A. Kenny [a,*]

[a] Department of Obstetrics and Gynecology, Section of Gynecologic Oncology, University of Chicago, Chicago, IL 60637, United States of America
[b] Department of Pathology, University of Chicago, Chicago, IL 60637, United States of America
[c] Department of Public Health Sciences, University of Chicago, Chicago, IL 60637, United States of America
[d] Cellular Screening Center, University of Chicago, Chicago, IL 60637, United States of America
[e] Department of Physiology, Cornell University Weill Medical College, New York, NY 10065, United States of America

HIGHLIGHTS

- Inhibition of fascin decreased migration of ovarian cancer cells.
- Inhibition of fascin decreased migration of human omental mesothelial cells.
- Inhibition of fascin decreased migration of human omental tumor cancer-associated fibroblasts.
- Inhibition of fascin *ex vivo* blocked ovarian cancer cell colonization of human omental tissue.
- Inhibition of fascin blocked OvCa metastasis *in vivo*.

ARTICLE INFO

Article history:
Received 29 November 2018
Received in revised form 15 January 2019
Accepted 20 January 2019
Available online 20 February 2019

Keywords:
Fascin
Ovarian cancer
Migration
Tumor microenvironment
Metastasis

ABSTRACT

Objective. Ovarian cancer (OvCa) metastasis requires the coordinated motility of both cancer and stromal cells. Cellular movement is a dynamic process that involves the synchronized assembly of f-actin bundles into cytoskeletal protrusions by fascin. Fascin directly binds f-actin and is an integral component of filopodia, lamellapodia and stress fibers. Here, we examine the expression pattern and function of fascin in the cancer and stromal cells of OvCa tumors.

Methods. Fascin expression was evaluated in human cells and tissues using immunohistochemistry and immunofluorescence. The functional role of fascin in cancer and stromal cells was assessed with *in vitro* functional assays, an *ex vivo* colonization assay and *in vivo* metastasis assays using siRNA/shRNA and an inhibitor. The effect of fascin inhibition on Cdc42 and Rac1 activity was evaluated using GTPase activity assays and immunofluorescence.

Results. Fascin expression was found to be higher in the stromal cell, when compared to the cancer cell, compartment of ovarian tumors. The low expression of fascin in the cancer cells of the primary tumor indicated a favorable prognosis for non-serous OvCa patients. *In vitro*, both knockdown and pharmacologic inhibition of fascin decreased the migration of cancer and stromal cells. The inhibition of fascin impaired Cdc42 and Rac1 activity in cancer cells, and cytoskeletal reorganization in the cancer and stromal cells. Inhibition of fascin *ex vivo* blocked OvCa cell colonization of human omental tissue and *in vivo* prevented and reduced OvCa metastases in mice. Likewise, knockdown of fascin specifically in the OvCa cells using a fascin-specific lentiviral-shRNA also blocked metastasis *in vivo*.

Conclusion. This study reveals the therapeutic potential of pharmacologically inhibiting fascin in both cancer and stromal cells of the OvCa tumor microenvironment.

1. Introduction

Despite its relatively low incidence, ovarian cancer (OvCa) is the fifth most common cause of cancer-associated mortality among women in the United States [1]. The relentless mortality rate of OvCa results

Abbreviations: OvCa, ovarian cancer; TMA, tissue microarray; HPMC, human primary mesothelial cells; CAF, cancer-associated fibroblasts.

* Corresponding authors.
E-mail addresses: elengyel@uchicago.edu (E. Lengyel), hkenny@uchicago.edu (H.A. Kenny).

https://doi.org/10.1016/j.ygyno.2019.01.020
0090-8258/

from wide-spread metastases to all mesothelium-lined organs in the peritoneal cavity (especially the pleura and abdominal cavity), which occurs in 75% of patients [2]. OvCa metastasis involves the key processes of cell adhesion, cell migration, cell invasion, cell proliferation and cellular interactions. These cellular processes require alterations in the actin cytoskeleton [3]. The actin-bundling protein, fascin, is a member of the cytoskeletal protein family. Fascin proteins organize f-actin into parallel bundles to produce filopodia, lamellapodia and stress fibers, which drive cell adhesion, cell migration and cellular interactions [4,5].

High fascin expression has been associated with increased mortality in breast, colorectal, and pancreatic carcinomas, and with metastasis in colorectal and gastric cancers [6,7]. The expression pattern of fascin in reproductive tissues and OvCa has been investigated in only three studies. These found that fascin is not expressed in the epithelial cells of the ovary or fallopian tube, but is expressed in epithelial OvCa tumors, and is most highly expressed in serous carcinomas [8,9]. A study of 89 patients with OvCa indicated no correlation between survival time and fascin expression levels; although, in a subgroup analysis of patients with FIGO stage III serous carcinomas ($n = 43$), overall survival in patients with tumors containing high fascin expression was significantly greater [8]. Conversely, a separate study of stage III poorly-differentiated serous carcinomas ($n = 56$) reported an inverse correlation between fascin expression and progression-free and overall survival [10].

Given existing data on the role of fascin in cancer cell movement and the critical role of the tumor stroma in promoting cancer metastasis, we hypothesized that fascin would also play a critical role in OvCa metastasis. Here, we report that inhibition of fascin *via* targeted siRNA/shRNA or inhibitor treatment decreased migration of OvCa cells, mesothelial cells, and cancer-associated fibroblasts (CAF) *in vitro* and reduced OvCa metastasis *in vivo*.

2. Methods

2.1. Reagents

The ovarian cancer cell lines HeyA8, Ovcar5, Tyk-nu, Snu119, and Kuramochi were provided by the University of Texas MD Anderson Cancer Center, University of California San Francisco, Osaka University Graduate School of Medicine, Korean Cell Line Bank, and the Japanese collection of Research Bioresources Cell Bank, respectively [11]. Hyaluronidase and collagenase type III were obtained from Worthington Biochemical (Lakewood, NJ). Lentiviral vector expressing copepod cGFP (pCDH-CMV-MCS-EF1, Cat# CD511B-1) was from Systems Biosciences (Palo Alto, CA). Fluorescently-labeled anti-mouse secondary antibodies and NP-40 were purchased from Fisher Scientific (Chicago, IL). Fascin antibody (clone 55K-2) for immunohistochemistry and immunofluorescence studies, and lentiviral shRNA (Catalog # SHCLNV TRCN0000123039) were from Sigma-Aldrich (St. Louis, MO). Fascin antibody (clone 55K-2) for immunoblots and paraformaldehyde (PFA) was acquired from Santa Cruz Biotechnology (Dallas, TX). The GAPDH antibody and horse-radish peroxidase linked anti-Mouse IgG were acquired from Cell Signaling Technology (Danvers, MA). GTP-Rac1 antibody was purchased from New East Biosciences (Malvern, PA). Fascin siRNA (Catalog #M-019576) was from Dharmacon (Lafayette, CO). The G-LISA Activation Assays for Cdc42 and Rac1, and the Cdc42 Pull-Down Activation Assay were purchased from Cytoskeleton, Inc. (Denver, CO). Hoechst 33342, Phalloidin-488, Lipofectamine 2000 Transfection Reagent, and fetal bovine serum were purchased from Thermo Fisher Scientific (Skokie, IL). G2 was synthesized by WuXi AppTech (Shanghai, China), and one batch of G2 was used in all *in vitro* and *in vivo* experiments [12]. G2 was also purchased from Xcessbio (San Diego, CA) to confirm *in vitro* findings.

2.2. Isolation and culture of primary human mesothelial cells and primary human cancer-associated fibroblasts

Normal human omental samples were acquired from female patients who underwent surgery and were free of cancer, endometriosis, or other inflammation. Omental tumor samples were acquired from patients with high-grade serous OvCa. Informed consent was obtained before the surgery and the study was approved by the IRB at the University of Chicago. The primary human mesothelial cells (HPMCs) were isolated from normal omentum. The CAFs were isolated from omental tumor of high-grade serous OvCa patients. The primary cells were cultured and characterized by vimentin, keratin 8, smooth-muscle actin, and calretinin immunohistochemistry [13–15]. Primary cells were used for experiments at passages 1–4 to minimize any divergence from original characteristics and morphology [14]. OvCa cells were fluorescently-labeled using a lentiviral vector expressing copepod cGFP as previously described [15].

2.3. Proteomic analysis

The MaxQB database (http://maxqb.biochem.mpg.de/mxdb/project/list) was queried using the Max Planck Perseus software for fascin expression in OvCa tumors from 11 patients and in 30 OvCa cell lines as previously described [11].

2.4. Immunohistochemistry

Human omental samples ($n = 3$) were acquired from female patients undergoing surgery for benign reasons. Omental metastases from 12 patients with high-grade serous OvCa were deparaffinized and incubated with anti-fascin antibody (1:2000 dilution) as previously described [16,17]. Slides were stained using the Envision avidin-biotin free detection system and counterstained with hematoxylin. Representative images were taken using a Leica Axiovert 200 inverted microscope with color camera.

2.5. Tissue microarray and immunohistochemistry

Tissue microarray (TMA) cores ($n = 2$, per patient sample) were constructed from primary OvCa and peritoneal and omental metastatic tissues collected from patients with OvCa ($N = 201$; $n = 153$ serous papillary, $n = 16$ clear cell, $n = 21$ endometrioid, and $n = 11$ mucinous). Clinical and histopathologic information was collected and updated every 3 months as previously reported [16]. TMA slides were deparaffinized and incubated with fascin antibody (1:2000 dilution) as previously described [16,17]. Slides were stained using the Envision avidin-biotin-free detection system and counterstained with hematoxylin. The intensity of 3, 3′-diaminobenzidine staining was determined in cancer- or stroma-specific regions of the tumor cores by a pathologist (AM) and given scores of 0 (absent), 1, 2 or 3 (highest). The score averages were reported.

2.6. Immunoblots

For analysis of fascin and GAPDH, cells were lysed, and equal quantities of protein for each sample were added to each blot. Proteins were resolved by SDS-PAGE, transferred to a nitrocellulose membrane, and immunoblot analysis was performed. Membranes were incubated with the following antibodies overnight at 4 °C: anti-fascin (1:1000 dilution), anti-GAPDH (1:2000 dilution). Blots were than incubated with secondary horseradish peroxidase–conjugated IgG and visualized with enhanced chemiluminescence reagents.

2.7. Short hairpin RNA (shRNA) and small interfering RNA (siRNA) fascin targeting

Fascin was stably knocked down in GFP/luciferase-labeled HeyA8 cells [15] using a lentiviral-based shRNA vector. The HeyA8 cells were plated in a 96-well plate (500 cells/well) in 10% fetal bovine serum, 1% MEM non-essential amino acids, 1% penicillin-streptomycin, 1% vitamins in DMEM (full growth media) and allowed to incubate overnight. The next day, cells were incubated in full growth media with 5 μg/ml hexadimethrine bromide and lentiviral particles at a multiplicity of infection of 2. After overnight incubation, media was removed and cells were selected for use in full growth media containing 1 μg/ml puromycin. Knockdown was confirmed by immunoblotting.

Fascin was transiently knocked down using fascin-targeting siRNAs. OvCa cells, HPMCs, and CAFs (3×10^5 cells/well) were transiently transfected with anti-fascin siRNA (5 nM) or control siRNA (5 nM)

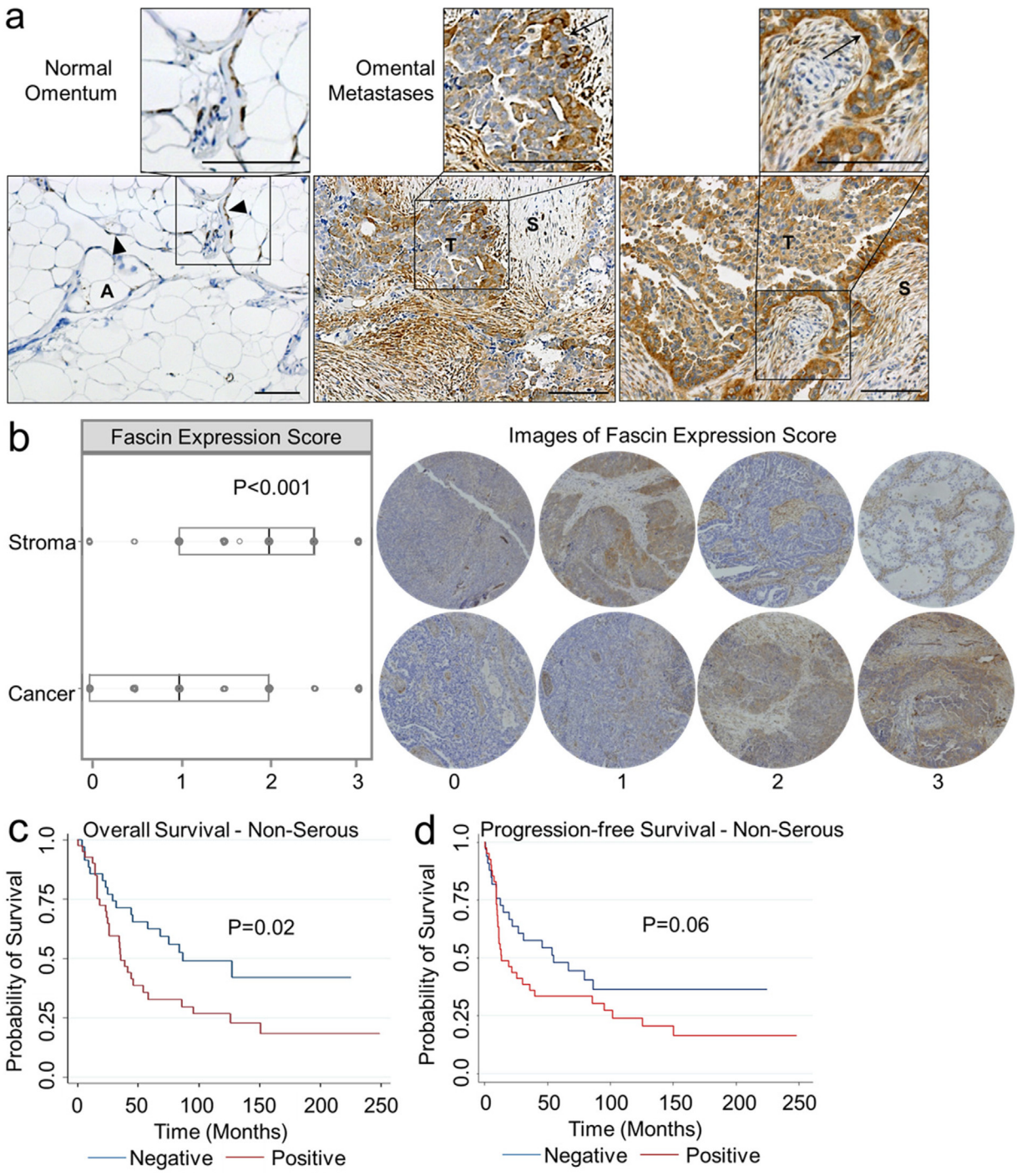

Fig. 1. Cancer and stromal cells express fascin protein in the ovarian cancer tumor microenvironment. a–c. Immunohistochemical analysis of fascin expression in formalin-fixed paraffin embedded tissues. a. Representative images of fascin expression in normal omentum and omental metastases. S, stroma. T, tumor. A, adipocytes. Arrows, tumor-stroma interface. Arrowhead, mesothelial cells. Size bar, 500 μm. b. Box plot analysis of fascin expression in the stroma or cancer compartment of all ovarian cancer tumor subtypes ($n = 201$) and representative images of immunohistochemistry scoring for stroma or cancer compartments in tumors. Boxes indicate 25th percentile, median, and 75th percentile. *** = $p < 0.001$ calculated from Wilcoxon signed-rank test. c–d. Kaplan-Meier analysis of overall survival (OS; $n = 76$ patients; c) and progression-free survival (PFS; $n = 74$ patients; d) across non-serous ovarian cancer subtypes in patients with 0 level (negative, blue, OS $n = 35$ patients, PFS $n = 33$ patients) fascin expression *versus* 1–3 level (positive, red, OS $n = 41$ patients, PFS $n = 41$ patients) fascin expression in cancer cells of primary tumor. *P*-values calculated from Cox regression analysis.

using Lipofectamine transfection reagent. After a six-hour incubation in transfection media, cells were incubated for 48 h in full growth media to ensure knockdown of fascin RNA and protein. Fascin knockdown was confirmed by western blot.

2.8. Migration assays

Boyden chamber cell migration assay: GFP-labeled OvCa cancer cells, HPMC's, or CAF's were added in serum-free media containing 50 μM G2 or DMSO (vehicle control) to the top well of 8 μM porous inserts. Full growth media containing 50 μM G2 or DMSO control was added to the bottom wells. Cells were allowed to migrate for 12-24 h. Non-migrated cells were removed from the top well using a cotton swab and migrated cells were fixed in 4% PFA and stained with crystal violet. Migrated cells were quantified in 5 random fields (excluding center and edges) at 200× magnification on Nikon Ti2 Eclipse fully-automated inverted fluorescence microscope.

Oris™ cell migration assay: This assay uses stopper barriers to create a central cell-free detection zone for cell migration experiments [18]. Briefly, 96-well plates were coated with rat-tail collagen 1 (2.5 μg/ml) and fibronectin (2.5 μg/ml). After incubation at 37 °C for 30 min, the ORIS stoppers (Platypus Technologies, Fitchburg, WI) were placed into wells. CAFs (10,000 cells/well) and/or GFP-labeled OvCa cells (15,000 cells/well) were added around the barriers. After a 12-h incubation at

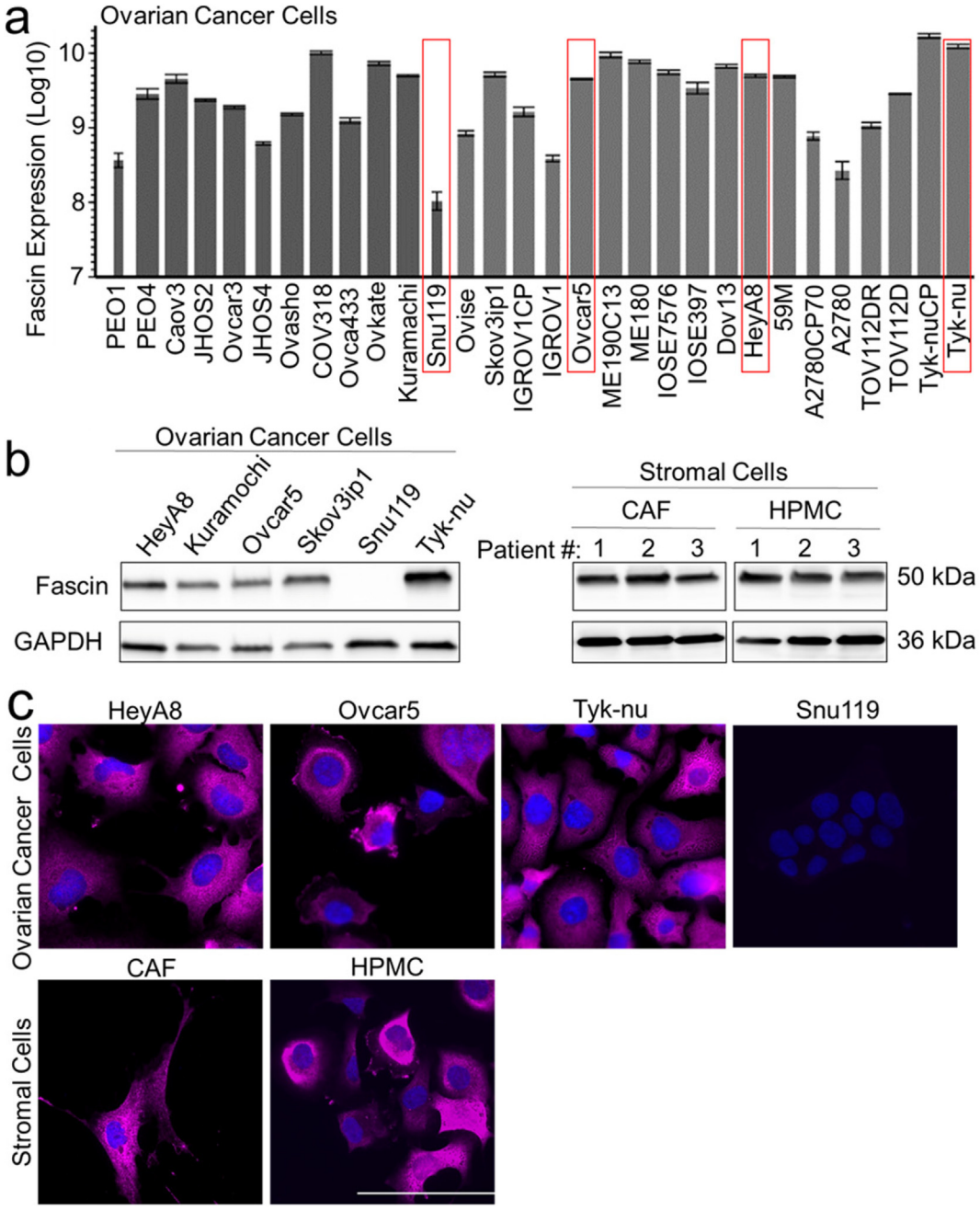

Fig. 2. Ovarian cancer cell lines, primary human omental tumor cancer-associated fibroblasts and omental mesothelial cells express fascin in culture. a. Protein expression level of fascin was determined by mass spectrometry in 30 ovarian cancer cell lines. The thickness of the bars indicate protein sequence coverage per sample (thicker = more coverage). The ovarian cancer cell lines used in experiments (red boxes). b. Immunoblot analysis of fascin expression in ovarian cancer cell lines (left panel), cancer-associated fibroblasts from omental metastases (CAF) and normal human primary omental mesothelial cells (HPMC; right panel). c. Immunofluorescent detection of fascin expression (pink) in ovarian cancer cell lines, CAFs and HPMCs. Blue, nuclei. Size bar, 20 μm. Bars represent mean ± standard deviation ($n = 3$).

37 °C, the barriers were removed and the media in each well was exchanged for fresh media containing either 10 μM G2 or DMSO control. Images were captured at $t = 0$ and 1 and 3 days after removal of stoppers and migrated cells were quantified using a fluorescent imaging cytometer, SpectraMax MiniMax 300 (Molecular Devices, San Jose, CA).

Wound healing migration assay: GFP-labeled OvCa cells were co-cultured with HPMC's and allowed to grow to 100% confluence in a 96-well plate, and then culture dishes were scratched using Woundmaker 96 (Essen Bioscience, Ann Arbor, MI). Cells were allowed to migrate into the scratched area of the dish for 8 h and were imaged using a Nikon Ti2 Eclipse fully-automated inverted fluorescence microscope with live imaging incubation chamber. At the end of the time course (16 h), total distance migrated was quantified for both HPMC's and OvCa cells using ImageJ. Movies of migration were captured on the fluorescent microscope using the live imaging chamber (5% CO_2 and 37 °C).

2.9. Ex-vivo full human omentum culture

Ex-vivo omental cultures were performed as described previously [16]. Briefly, a fresh piece of full human omentum was cut into 8 mm pieces (equivalent weights) and placed in a 24-well dish (1 piece/well). GFP-labeled HeyA8, Ovcar5, or Tyk-nu cells (1×10^6 cells/well) were added to the omentum and incubated at 37 °C in full growth media containing 10 μM G2 for 24 h. After incubation, omental pieces were washed 3 times in PBS, digested in 5% NP-40 for 30 min at 37 °C, and scraped with a metal spatula. All cells removed during digestion were placed in a 24-well plate, and the total fluorescent intensity per well was quantified.

2.10. Immunofluorescence and phalloidin staining

Cells were plated on glass bottom 96-well plates and grown for 24 h before treatment with G2 (50 μM) or DMSO (vehicle control) for 8 h. The cells were fixed in 4% PFA, permeabilized in TBS with 0.1% triton-X and blocked in TBS containing 10% goat serum, 1% BSA, and 0.1% triton-X (blocking buffer) for 1 h. Primary antibodies against fascin (1:300 dilution) or GTP-Rac1 (1:300) were added to blocking buffer and incubated overnight at 4 °C. The wells were washed with TBS containing 0.1% triton-x and incubated with secondary antibody mixture (anti-mouse fluorescently-labeled secondary). Actin was stained with Phalloidin-488 according to manufacturer instructions (Invitrogen, Carlsbad, CA). A nuclear counterstain was performed with Hoechst. Imaging was performed using a Nikon Ti2 Eclipse fully-automated inverted fluorescence microscope.

2.11. GTPase activity of Cdc42 and Rac1

HeyA8 cells (5×10^6) were plated on a 150 mm culture dish for 24 h, and treated with 50 μM G2 for 5 h in serum-free media. Ten minutes before the cells were lysed, they were treated with 50 ng/ml epidermal growth factor (EGF) to activate Cdc42 and Rac1. Cells were washed with PBS, lysed, scraped, collected, and pelleted. Following the cell harvest, total protein concentration was detected with BCA Protein Assay (ThermoFisher Scientific). For G-LISA Cdc42 and Rac1,2,3 Activation Assay Biochem Kit (colorimetric format), equal amounts of protein were added to each well of G-LISA plates and the assay performed according to manufacturer instructions (Cytoskeleton Inc., Denver, CO) and as previously described [16]. For the Cdc42 pulldown assay (Cell Biolabs Inc., San Diego, CA) the immunoprecipitation – immunoblot was performed as previously described [16], the lysates was incubated with 0.05 M EDTA for 30 min at 30 °C. GTPγS or GDP were added to duplicate samples for positive and negative controls, and loading was quenched with 0.2 M $MgCl_2$ treatment.

2.12. In vivo experiments

Omental colonization: GFP/luciferase-labeled HeyA8 cells (1×10^6 cells) were co-injected with 100 mg/kg of G2. An additional dose of G2 was given intraperitoneally (IP) 48 h after injection. On day 4 post HeyA8 injection, mice were sacrificed. Representative immunofluorescence images of the omental tissue were captured using fluorescent microscope (Nikon), omental lysates were prepared, and total luciferase activity was quantified as described previously [19].

Metastasis: Fascin was stably knocked down in GFP/luciferase-labeled HeyA8 cells [15] using a lentiviral-based shRNA vector (described above). The HeyA8 OvCa cells (0.5×10^6) were injected IP into athymic nude mice (Harlan, Indianapolis, IN). The control group mice were injected with HeyA8 cells infected with a control shRNA construct. On day 21, mice were sacrificed, tumors were dissected and metastatic tumor burden was quantified [17].

Intervention treatment: The GFP-labeled HeyA8 OvCa cells (0.5×10^6) were injected IP into athymic nude mice (Harlan, Indianapolis, IN). The mice received daily IP injections of G2 at 100 mg/kg body weight on days 8–21 post-HeyA8 injection. The control group was treated with DMSO (vehicle control). On day 21, mice were sacrificed, tumors were dissected and metastatic tumor burden was quantified.

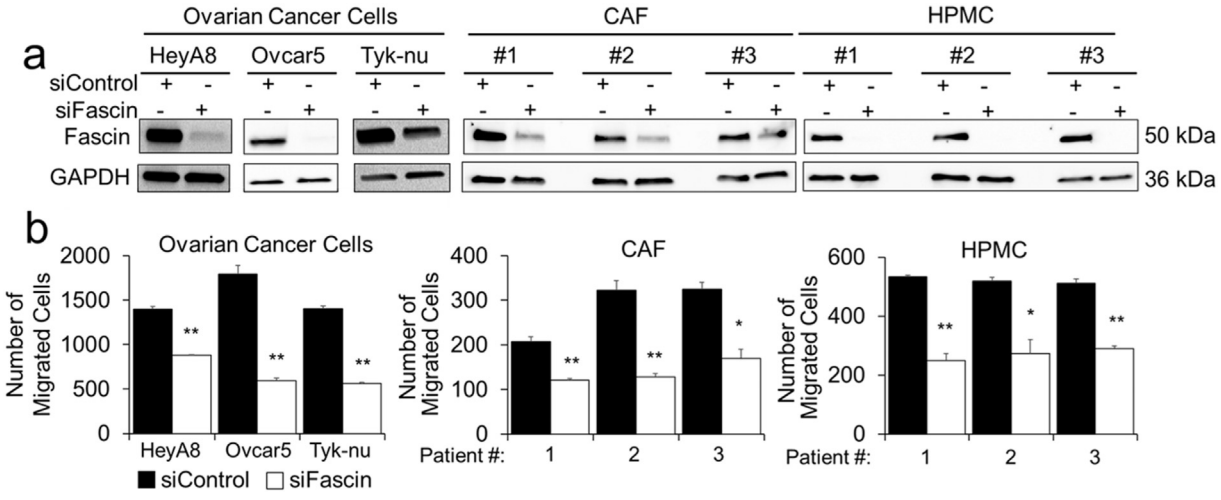

Fig. 3. Knockdown of fascin decreases migration of ovarian cancer and stromal cells. a. Immunoblot analysis of fascin and GAPDH protein levels in HeyA8, Ovcar5, and Tyk-nu ovarian cancer cells, primary human cancer-associated fibroblasts (CAF) and primary human omental mesothelial cells (HPMC) 72 h after siRNA transfection. b. Boyden chamber migration assay for HeyA8, Ovcar5, and Tyk-nu ovarian cancer cells, CAF and HPMC cells transfected with control or fascin siRNA. Bars represent mean ± standard error of the mean ($n = 5$ fields, $n = 5$ wells per cell type; $n = 3$ independent experiments). * = $p < 0.05$ and ** = $p < 0.01$ calculated using a two-tailed paired *t*-test.

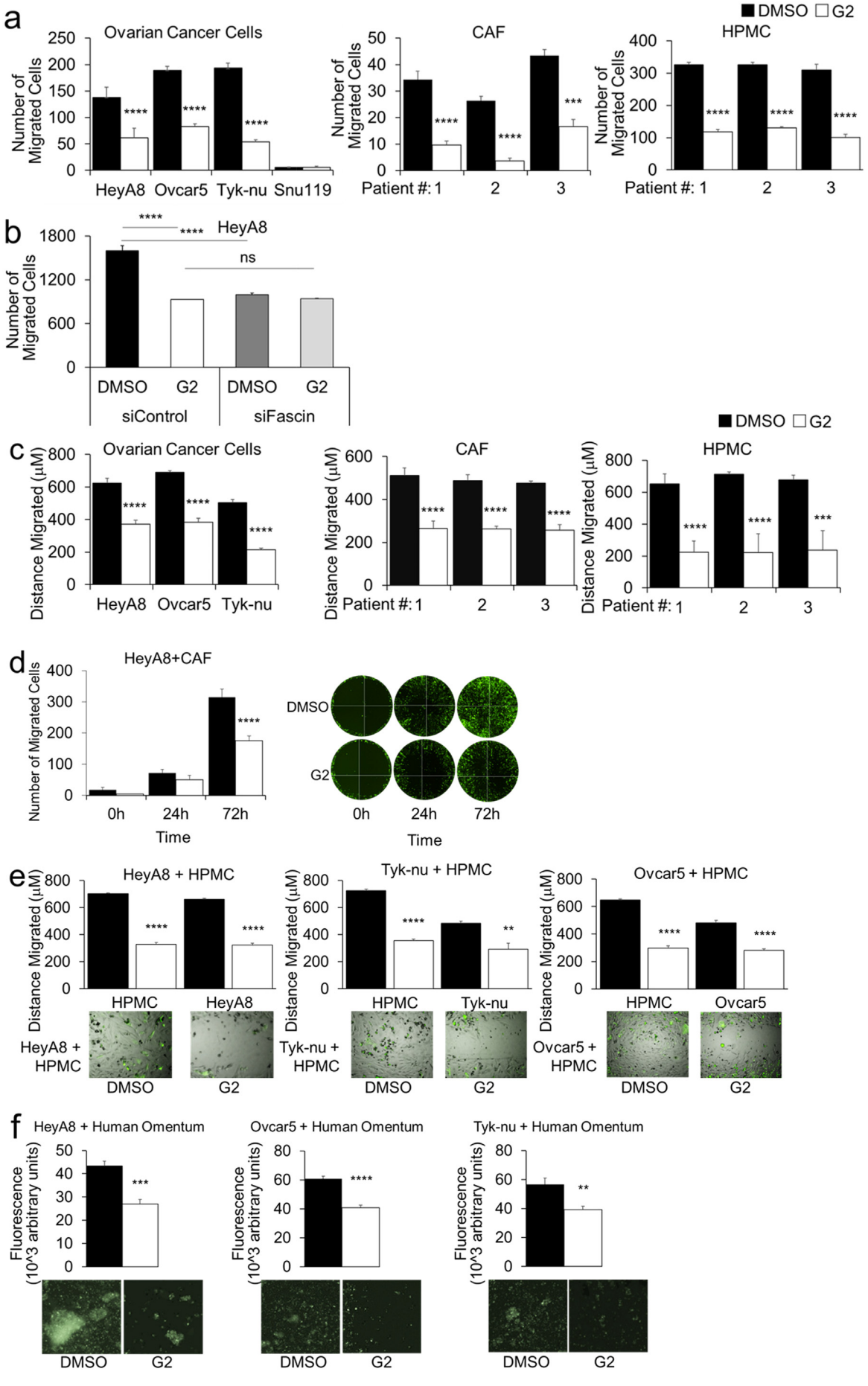
a
DMSO G2
Ovarian Cancer Cells
Number of Migrated Cells
HeyA8 Ovcar5 Tyk-nu Snu119
CAF
Patient #: 1 2 3
HPMC
b
HeyA8
ns
DMSO G2 DMSO G2
siControl siFascin
c
Distance Migrated (μM)
Ovarian Cancer Cells
HeyA8 Ovcar5 Tyk-nu
CAF
HPMC
d
HeyA8+CAF
Number of Migrated Cells
0h 24h 72h
Time
DMSO
G2
e
HeyA8 + HPMC
Tyk-nu + HPMC
Ovcar5 + HPMC
HPMC HeyA8
HPMC Tyk-nu
HPMC Ovcar5
HeyA8 + HPMC
Tyk-nu + HPMC
Ovcar5 + HPMC
f
HeyA8 + Human Omentum
Ovcar5 + Human Omentum
Tyk-nu + Human Omentum
Fluorescence (10^3 arbitrary units)

2.13. Statistical analysis

Statistical differences in fascin expression in the tumor compared to stroma were calculated from Wilcoxon signed-ranked test. Overall and progression-free survival estimates were computed using the Kaplan-Meier method, and comparisons between groups were analyzed using Cox regression. These analyses were performed using Stata (StataCorp, College Station, TX). To determine differences between experimental groups, unpaired/two-sample *t*-tests were used for *in vivo* experiments and two-tailed paired t-tests were used for *in vitro* experiments employing Microsoft Excel.

An outline of the study design and results are listed in Supplementary Table 1.

3. Results

3.1. Fascin is expressed in cancer and stromal cells of human ovarian tumors

Because the role of fascin during OvCa metastasis has not been explored, the expression pattern of fascin in normal omental tissue and OvCa omental metastases was defined. Fascin staining of six normal omental tissue samples showed fascin expression in the omental mesothelial cells (Fig. 1a, left). In 12 high-grade serous OvCa omental metastases, strong fascin expression was detected in both the stroma and the cancer cells located at the tumor-stroma interface (Fig. 1a, middle and right). The MaxQB database was queried for fascin expression in OvCa tumors from 11 patients, and the stromal compartment had higher levels of fascin when compared to the epithelial cell compartment of OvCa tumors from the ovary and omentum (data not shown). Given these initial findings, we sought to quantify fascin expression in the cancer cell and stromal cell compartments of primary and metastatic tumors using a tissue microarray (TMA) containing tissue sections from 201 patients with OvCa (Fig. 1b). Fascin was expressed in the cancer compartment of the tumor in 125/201 (62.2%) and in almost every case in the stromal cell compartment (189/201, 94.0%) (Supplementary Table 2). In all OvCa tumors, the stromal compartment had significantly higher levels of fascin expression (median 2.0) when compared to the cancer compartment (median 1.0; Fig. 1b). Fascin expression was correlated with pathology sub-type, age at diagnosis and FIGO stage at diagnosis (Supplementary Table 3). Despite the finding that serous OvCa had the highest levels of fascin expression, no significant correlation between fascin levels and overall survival or progression-free survival was found in patients with serous OvCa (Supplementary Fig. 1a and 1b). However, fascin expression was associated with worse overall survival (Fig. 1c), but not progression-free survival (Fig. 1d) in non-serous OvCa. Similar levels of fascin were quantified in primary *versus* metastatic tumors (data not shown).

The MaxQB database was queried for fascin expression in 30 common OvCa cell lines previously identified and published by our group [11], and fascin protein was detected in the thirty cell lines analyzed (Fig. 2a). Immunoblot (Fig. 2b) [11,20] and immunofluorescent (Fig. 2c) analysis of fascin expression corroborated the proteomic findings in both high-grade serous (Kuramochi, Snu119, Tyk-nu) and non-serous (Skov3ip1, HeyA8, Ovcar5) OvCa cell lines. We next determined if the stromal compartment cells, primary HPMCs from omentum and primary human CAFs from OvCa omental tumors, continue to express fascin when isolated and cultured. Both immunoblot (Fig. 2b) and immunofluorescent analysis (Fig. 2c) showed fascin expression in HPMC and CAF cells cultured from multiple patients.

3.2. Targeted fascin inhibition using siRNA and G2 decreases OvCa, HPMC, and CAF migration in vitro

Next, we assessed the effect of fascin-targeting small-interfering RNAs (siRNAs) on cellular function in OvCa, HPMC, and CAF cells (Fig. 3a). Using the Boyden chamber migration assay, we found that fascin knockdown decreased the migration all the cell types tested. (Fig. 3b). In previous studies with migrating breast and colon cells, the small-molecule compound G2, and its analogs, were found to directly bind fascin and block it from binding to actin filaments, consequently preventing the formation of filopodia, lamellapodia, and stress fibers. [21–23]. Therefore, we explored the effect of fascin inhibition with G2 in OvCa, HPMC, and CAF cell migration using the Boyden chamber migration assay. G2 treatment decreased individual cell migration of HeyA8, Ovcar5, and Tyk-nu OvCa cells, as well as HPMCs and CAFs (Fig. 4a). Of note, Snu119 OvCa cells, which lack fascin expression, did not migrate, regardless of treatment (Fig. 4a). In order to confirm that G2 specifically targeted fascin when inhibiting cancer cell migration, the effect of G2 on the migration of cancer cells that lacked fascin was evaluated. In a migration assay, G2 treatment had no effect on the migration of HeyA8 cells transfected with fascin-targeting siRNAs, indicating that G2 acts through fascin in the inhibition of OvCa cell migration (Fig. 4b). In a wound healing migration assay, G2 blocked the migration of OvCa cells, HPMCs and CAFs. (Fig. 4c). Furthermore, G2 significantly inhibited the migration of fluorescently-labeled HeyA8 cells that were co-cultured with CAFs or HPMCs (Fig. 4d) and also significantly inhibited the co-migration of HPMC and HeyA8, Tyk-nu and Ovcar5 cells (Fig. 4e and Supplementary Videos 1–6). To evaluate the *in vivo* situation encountered by OvCa cells, fluorescently-labeled OvCa cells were added with G2 to full human omentum, cultured *ex vivo* for 16 h, enzymatically digested, and their total fluorescence measured as previously described [24]. Treatment with G2 significantly inhibited HeyA8, Ovcar5 and Tyk-nu cell colonization of the human omentum (Fig. 4f).

To learn if other aspects of metastasis are affected by fascin knockdown or inhibition we evaluated cellular adhesion, invasion, proliferation, viability, and apoptosis as previously described [25]. Inhibition of fascin by siRNA or using the G2 inhibitor had no effect on adhesion, invasion or proliferation of 3 cancer cell lines through the 3D omental culture (Supplementary Figs. 2a–b, 3a–b and 4a–b). Similarly, inhibition of fascin by siRNA or G2 had no effect on HPMC or CAF invasion through collagen type 1 (Supplementary Fig. 3c), co-invasion of HeyA8 and CAF cells (Supplementary Fig. 3d) or HPMC cell proliferation (Supplementary Fig. 4a–b). G2 treatment also had no effect on OvCa cell viability or apoptosis (Supplementary Fig. 4c–d), indicating that the reduction in cell migration following fascin inhibition was not due to a decrease in cell proliferation or cell death. Collectively, these experiments suggest that fascin inhibition acts to decrease migration of both cancer and stromal cells.

Fig. 4. Treatment with G2, a fascin inhibitor, decreases migration of ovarian cancer and stromal cells. a. Boyden chamber migration assay for HeyA8, Ovcar5, and Tyk-nu ovarian cancer cells (left panel), primary human cancer-associated fibroblasts (CAF; middle panel) and primary human omental mesothelial cells (HPMC; right panel) treated with 50 μM G2 or DMSO control. ($n = 5$ fields per well, $n = 3$ wells per cell type; $n = 3$ independent experiments). b. Boyden chamber migration assay for HeyA8 ovarian cancer cells transfected with control or fascin siRNA and treated with 50 μM G2 or DMSO control. c. Wound healing assay for HeyA8, Ovcar5, and Tyk-nu ovarian cancer cells (left panel), primary human cancer-associated fibroblasts (CAF; middle panel) and primary human omental mesothelial cells (HPMC; right panel) treated with 50 μM G2 or DMSO control. ($n = 5$ wells per cell type; $n = 3$ independent experiments). d. Oris plug migration assay for HeyA8 cells co-cultured with cancer-associated fibroblasts (CAF) and treated with 10 μM G2 or DMSO control for 72 h. ($n = 6$ wells per treatment group; data shown is representative of 2 independent experiments). Representative fluorescent images of GFP-labeled HeyA8 ovarian cancer cell migration at 0, 24, and 72 h. e. Wound healing assay for HeyA8, Ovcar5, and Tyk-nu ovarian cancer cells in co-culture with primary human omental mesothelial cells (HPMC) treated with 50 μM G2 or DMSO control. ($n = 5$ wells per cell type; $n = 3$ independent experiments). Representative fluorescent images 24 h after wound healing assay of GFP-labeled ovarian cancer cells and unlabeled primary human mesothelial cells. f. *Ex-vivo* primary human omental tissue colonization assay using HeyA8, Ovcar5, and Tyk-nu ovarian cancer cells for 16 h with 50 μM G2 or DMSO control. ($n = 5$ tissues from same patient per cell type; $n = 2$ independent experiments). Bars represent mean ± standard error of the mean. Differences between treatments were evaluated using a paired *t*-test, two-tailed, with $p < 0.01$ (**), $p < 0.001$ (***), $p < 0.0001$ (****).

3.3. G2 decreases the activation of Cdc42 and Rac1

Cdc42 and Rac1 are two Ras-related Rho family of GTP-binding proteins that support a migratory phenotype in cells and regulate fascin [26]. Therefore, we explored the effect of fascin inhibition on f-actin structure as well as GTPase activity of Cdc42 and Rac1 (Fig. 5). F-actin fibers were low to absent in the OvCa and HPMC co-cultures after treatment with G2 and the cells had no evidence of filopodia or

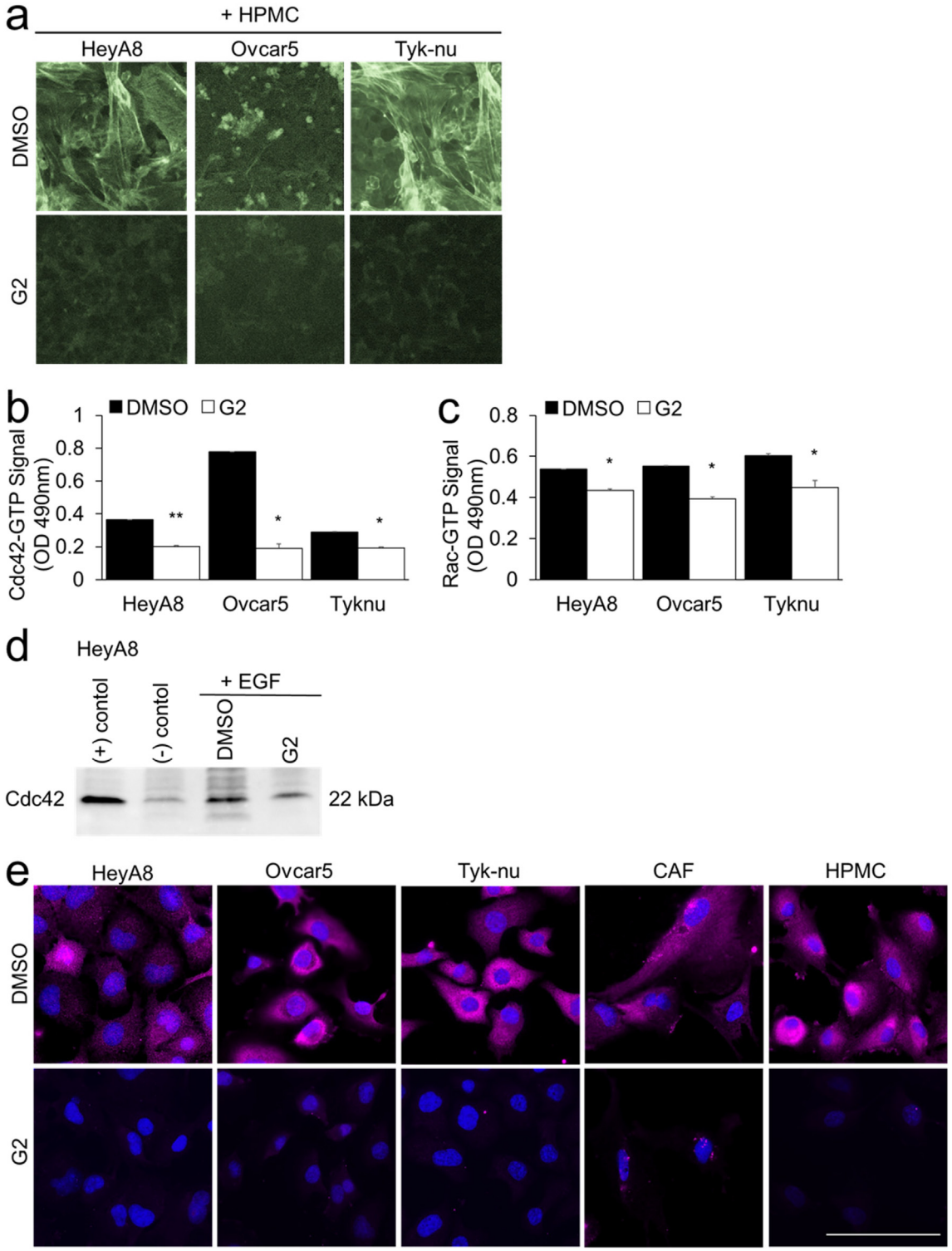

Fig. 5. Treatment with G2, a fascin inhibitor, decreases actin bundling, Cdc42-GTP and Rac1-GTP activity in both cancer and stromal cells. a. F-actin (Phalloidin-488) and nuclear (Hoechst) staining of cancer cells and primary human mesothelial cells (HPMC) after 24 h co-culture and subsequent 8 h of treatment with 50 μM G2 or DMSO (vehicle control). b-e. Cancer cells were cultured on plastic. Twenty-four hours later the cancer cells were treated for 5 h with 50 μM G2 or DMSO control in serum-free media followed by 10 min treatment with 50 ng/ml epidermal growth factor (EGF). The levels of GTP-bound Cdc42 or Rac1 were measured using the following assays. b. Cdc42 G-LISA Activation Assay. c. Rac1,2,3 G-LISA Activation Assay. Bars represent mean ± standard error of the mean ($n = 5$ wells per cell type; $n = 3$ independent experiments). Differences between treatments were evaluated using a paired t-test, two-tailed, with $p < 0.05$ (*) and $p < 0.01$ (**).d. Cdc42 Pull-down Activation Assay. e. Immunofluorescent detection of Rac1-GTP (pink). Blue, nuclei. Size bar, 50 μm.

lamellipodia (Fig. 5a). The levels of GTP-bound Cdc42 and Rac1,2,3 were determined by G-LISAs (Fig. 5b–c), a Cdc42 immunoprecipitation immunoblot activity assay (Fig. 5d) and immunofluorescence with a GTP-Rac1 specific antibody (Fig. 5e). Both GTP-Cdc42 and GTP-Rac1 levels were decreased following treatment with G2 (Fig. 5b–e). No change in GTP-Rac1 intracellular localization was detected in cancer and stromal cells with G2 treatment. Collectively, these experiments suggest that fascin inhibition decreases the GTPase activity of both Cdc42 and Rac1.

3.4. G2 blocks metastatic disease burden in vivo

Given the positive *in vitro* studies, we next investigated the effect of inhibiting fascin on early and late OvCa metastasis *in vivo*. First, we generated stable populations of HeyA8 cells expressing lentivirus-derived shRNA targeting fascin (Fig. 6a). After IP injection of cancer cells into athymic nude mice, tumor burden was quantified after 21 days. The intraperitoneal injection of HeyA8-shFascin cells led to smaller tumors, but the number of metastases was unchanged (Fig. 6a). There was a

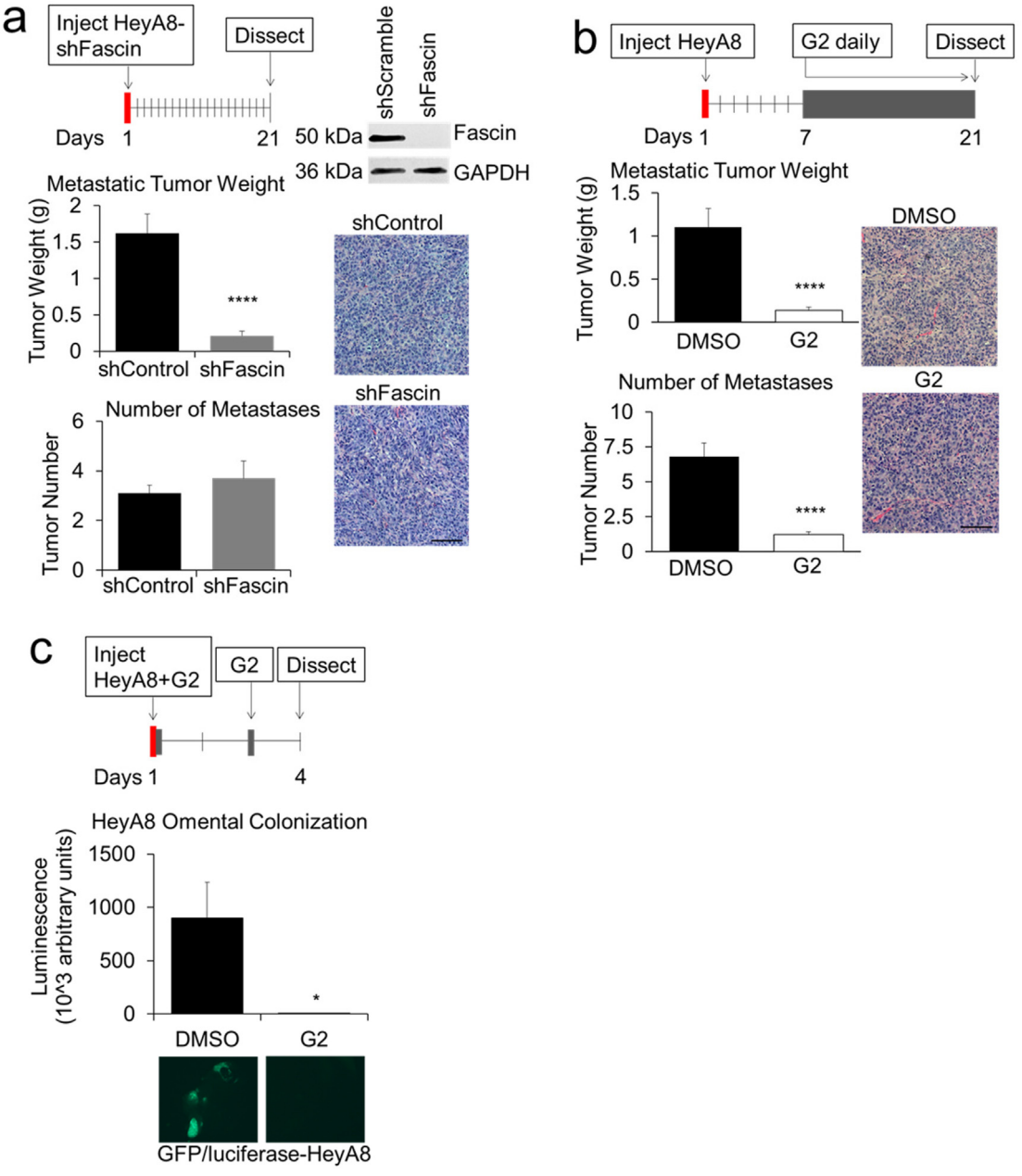

Fig. 6. Knockdown of fascin in ovarian cancer cells or in-vivo treatment with G2, a fascin inhibitor, decreases ovarian cancer metastasis. a–c. HeyA8 ovarian cancer xenograft models of metastasis. a. Metastasis assay. HeyA8 cells were infected with lentiviral control (shControl) or fascin-specific shRNA particles (shFascin). Top right, immunoblot analysis of fascin protein expression in the infected cells. Mice were injected intraperitoneally (IP) with infected cells (1×10^6) and tumors were harvested 21 days post-injection. Metastatic tumor weight (top graph) and tumor number (lower graph) were quantified. Images on right are representative of the HeyA8 tumors stained with hematoxylin and eosin. b. Intervention treatment assay. Mice were treated with daily IP injections of G2 (2 mg/mouse/day) or DMSO control beginning 7 days after injection of HeyA8 (1×10^6) OvCa cells. Twenty-one days post HeyA8 injection, tumors were harvested and metastatic tumor weight (top graph) and number of tumors (bottom graph) were quantified. Images on right are representative of the HeyA8 tumors stained with hematoxylin and eosin. c. Omental colonization assay. GFP/luciferase-labeled HeyA8 cells (1×10^6) were co-injected and treated IP 48 h after injection with 10 μM G2 or DMSO control. Forty-eight hours later mice were treated with G2 (2 mg/mouse) IP. Four days post cancer cell injection, the omentums were collected. Relative luminescent units in total omental lysates were detected using a luminescence assay. Bars represent mean ± standard error of the mean ($n = 5$ mice per treatment group). Representative fluorescent images of ovarian cancer cell colonization on mouse omentum are shown. * = $p < 0.05$ and **** = $p < 0.0001$ calculated using an unpaired/two-sample *t*-test.

small but significant increase in the proportion of Ki67 (proliferation) and cleaved-caspase 3 (apoptosis) positive cells in the HeyA8-shFascin tumors, but no differences in CD31 (angiogenesis). (Supplementary Fig. 5a). In order to assess the therapeutic potential of G2, tumors were allowed to establish for seven days prior to daily IP injections of G2 (Fig. 6b). The treatment with G2 significantly reduced tumor weight and tumor number, suggesting an effect on late metastasis. There were no differences in intra-tumoral proliferation, apoptosis or angiogenesis (Supplementary Fig. 5b). To assess the role of G2 in early cancer cell colonization, HeyA8 cells were co-injected with G2, an additional dose of G2 was given IP 48 h later, and the omentum was collected in another 48 h [24]. Treatment with G2 also significantly reduced HeyA8 omental colonization, suggesting an effect on early metastasis (Fig. 6c).

4. Discussion

One of the hallmarks of cancer metastasis is the coordinated migration and invasion of both cancer and stromal cells. During the early phases of metastasis, this involves complex, dynamic processes that require the continuous remodeling of the cellular cytoskeleton to adapt to challenges of fast growth and an initially hostile tumor microenvironment at the metastatic site. Fascin, the actin bundling protein, regulates the formation and maintenance of filopodia, lamellipodia, and stress fibers, which play a critical role during migration and early metastasis [4,5,27].

Our experiments in OvCa metastasis found several lines of evidence that support an important role for fascin. OvCa metastasis was inhibited when fascin was knocked down in OvCa cells and was prevented and blocked in mice when fascin was therapeutically targeted prior to metastasis formation. Furthermore, treatment with G2 after OvCa metastasis very efficiently reduced the metastatic tumor burden in mice. These data complement previous reports in other cancers that metastasize within the peritoneal cavity. Knockdown of fascin in cancer cells decreased tumor growth and metastasis in murine models of gastric, pancreatic and colon cancers [7,28]. A fascin siRNA in gastric cancer cells decreased the number of metastases after intra-peritoneal injection by 60% [29]. In a transgenic model of pancreatic cancer, fascin-deficient mice had longer survival times, delayed onset of cancer, and had a lower tumor burden than mice expressing fascin [7]. Last, in a xenograft model of colon cancer, doxicillin-induced knockdown of fascin resulted in decreases in primary tumor growth and the number of metastases [28]. These studies clearly show that cancer growth and metastasis are fascin-dependent in ovarian, gastric, pancreatic, colon and breast cancers. They also support the clinical conclusion reached after a meta-analysis of 25 immunohistochemical studies of five epithelial cancers. This analysis found that fascin-1 protein expression is associated with lymph node and distant metastasis and, on average, a 44% increased risk of death [6].

When we stained all ovarian cancer histologic subtypes using a TMA, we found that fascin protein expression was correlated with advanced stage cancer, and that fascin levels were significantly higher in high-grade serous tumors. However, fascin expression was only correlated with poor overall survival in non-serous epithelial ovarian cancers. A possible explanation for this finding is that the endometrioid, clear cell, and mucinous subtypes grow in a more invasive pattern, leading to deeper invasion and distant metastasis, while the high grade subtype only superficially attaches to the peritoneum and is often much easier to remove from the underlying anatomical structures. We detected the highest expression of fascin at the invasive edge of high-grade serous tumors, where cancer and stromal cells interact and engage in bi-directional signaling [30]. An interesting direction for future studies will be to determine if cancer cells directly reprogram the cytoskeleton of stromal cells through specific cytokines or if the reorganization of the cytoskeleton is a global reaction of stromal cells to a changed microenvironment.

Other groups have noted that fascin is expressed in the tumor stroma of ovarian epithelial [31] and colorectal [32] carcinomas. We also found fascin expression in both the tumor and stroma, and show that fascin is statistically higher in the stromal compartment than in the cancer compartment of OvCa tumors. These findings raise the possibility that targeting both compartments may be an effective therapeutic strategy.

Treatment with G2 led to a decrease in both GTP-bound Cdc42 and Rac1 that was concomitant with the absence of actin bundling into stress fibers and cellular migration. Rho GTPases, as well as fascin, are frequently up-regulated in migrating cells. The Rho GTPases, including Cdc42 and Rac1, induce fascin localization to filopodia and lamellipodia and their subsequent formation [33,34]. Therefore, this data further support the use of G2 for specifically targeting fascin functions. A regulation of Rac activity by fascin has also been previously observed in colon cancer cells, where knockdown of fascin resulted in decreased GTP-bound fascin and decreased Rac-dependent migration on laminin [28].

In summary, the coordinated migration of both ovarian cancer and stromal cells is blocked by inhibiting fascin and the inhibition of migration by a fascin inhibitor impeded the early phases of metastasis *in vivo*. We believe that, together with previous studies, our study indicates that fascin could be targeted in early metastasizing ovarian tumors, and that fascin expression is a potential marker of poor prognosis in non-epithelial ovarian cancers. However, the prognostic significance of fascin in high-grade serous OvCa remains inconclusive, and should be examined in larger studies.

Supplementary data to this article can be found online at https://doi.org/10.1016/j.ygyno.2019.01.020.

Acknowledgements

We thank Gail Isenberg and Mark Eckert for editing the manuscript. This work was supported by The University of Chicago Pritzker School of Medicine Summer Research Program (SM), R01CA111882 (EL), Ovarian Cancer Research Fund Alliance - Liz Tilberis Early Career Award 545674 (HAK), and Bears Care, the charitable beneficiary of the Chicago Bears Football Club (HAK & EL). We thank the Cellular Screening Center and Human Tissue Resource Center Cores at the University of Chicago, which are funded by the Cancer Center Support Grant (P30CA014599).

Author contribution

Conception and design: E. Lengyel, H.A. Kenny.

Development of methodology: S. McGuire, H.A. Kenny.

Acquisition of data (provided animals acquired and managed patients, provided facilities, *etc.*): B. Kara, P.C. Hart, S. Fazal, H.A. Kenny.

Analysis and interpretation of data (*e.g.*, statistical analysis, biostatistics, computational analysis): S. McGuire, A. Montag, K. Wroblewski, H.A. Kenny.

Writing, review, and/or revision of the manuscript: S. McGuire, E. Lengyel, H.A. Kenny.

Administrative, technical, or material support (*i.e.*, reporting or organizing data, constructing databases): X.-Y. Huang, E. Lengyel.

Study supervision: E. Lengyel, H.A. Kenny.

Conflict of interest

X.-Y. Huang is a co-founder and has equity in Novita Pharmaceuticals. Ms. Wroblewski reports a grant from NCI during the conduct of the study. Dr. Lengyel reports grants from Bears Care and NCI during the conduct of the study, and a grant from Abbvie Inc. outside the submitted work. Dr. Kenny reports grants from Bears Care and the Ovarian Cancer Research Fund Alliance during the conduct of the study, and a grant from Abbvie Inc. outside the submitted work. S. McGuire, P.C. Hart, B. Kara and S. Fazal have no conflicts of interest. Unfortunately A. Montag has passed away, but to the best of the knowledge of all co-authors, he had no conflicts of interest to declare.

E. Lengyel dedicates this manuscript to the memory of Dr. Anthony Montag, a brilliant gynecologic pathologist and great collaborator.

References

[1] R.L. Siegel, K.D. Miller, A. Jemal, Cancer statistics, 2018, CA Cancer J. Clin. 68 (2018) 7–30, https://doi.org/10.3322/caac.21442.

[2] E. Lengyel, Ovarian cancer development and metastasis, Am. J. Pathol. 177 (2010) 1053–1064, https://doi.org/10.2353/ajpath.2010.100105.

[3] J.J. Bravo-Cordero, L. Hodgson, J. Condeelis, Directed cell invasion and migration during metastasis, Curr. Opin. Cell Biol. 24 (2012) 277–283, https://doi.org/10.1016/j.ceb.2011.12.004.

[4] D. Vignjevic, S. Kojima, Y. Aratyn, O. Danciu, T. Svitkina, G.G. Borisy, Role of fascin in filopodial protrusion, J. Cell Biol. 174 (2006) 863–875, https://doi.org/10.1083/jcb.200603013.

[5] N. Kureishy, V. Sapountzi, S. Prag, N. Anilkumar, J.C. Adams, Fascins, and their roles in cell structure and function, Bioessays 24 (2002) 350–361, https://doi.org/10.1002/bies.10070.

[6] V.Y. Tan, S.J. Lewis, J.C. Adams, R.M. Martin, Association of fascin-1 with mortality, disease progression and metastasis in carcinomas: a systematic review and meta-analysis, BMC Med. 11 (2013), 52. https://doi.org/10.1186/1741-7015-11-52.

[7] A. Li, J.P. Morton, Y. Ma, S.A. Karim, Y. Zhou, W.J. Faller, E.F. Woodham, H.T. Morris, R.P. Stevenson, A. Juin, N.B. Jamieson, C.J. MacKay, C.R. Carter, H.Y. Leung, S. Yamashiro, K. Blyth, O.J. Sansom, L.M. Machesky, Fascin is regulated by slug, promotes progression of pancreatic cancer in mice, and is associated with patient outcomes, Gastroenterology 146 (1386-96) (2014) e1–17, https://doi.org/10.1053/j.gastro.2014.01.046.

[8] L.C. Hanker, T. Karn, U. Holtrich, M. Graeser, S. Becker, J. Reinhard, E. Ruckhaberle, H. Gevensleben, A. Rody, Prognostic impact of fascin-1 (FSCN1) in epithelial ovarian cancer, Anticancer Res. 33 (2013) 371–377.

[9] S.H. Park, J.-Y. Song, Y.-K. Kim, J.H. Heo, H. Kang, G. Kim, H.J. An, T.H. Kim, Fascin1 expression in high-grade serous ovarian carcinoma is a prognostic marker and knockdown of fascin1 suppresses the proliferation of ovarian cancer cells, Int. J. Oncol. 44 (2014) 637–646, https://doi.org/10.3892/ijo.2013.2232.

[10] A. Daponte, E. Kostopoulou, C.N. Papandreou, D.D. Daliani, M. Minas, G. Koukoulis, I.E. Messinis, Prognostic significance of fascin expression in advanced poorly differentiated serous ovarian cancer, Anticancer Res. 28 (2008) 1905–1910.

[11] F. Coscia, K.M. Watters, M. Curtis, M.A. Eckert, C.Y. Chiang, S. Tyanova, A. Montag, R.R. Lastra, E. Lengyel, M. Mann, Integrative proteomic profiling of ovarian cancer cell lines reveals precursor cell associated proteins and functional status, Nat. Commun. 7 (2016), 12645. https://doi.org/10.1038/ncomms12645.

[12] F.K. Huang, S. Han, B. Xing, J. Huang, B. Liu, F. Bordeleau, C.A. Reinhart-King, J.J. Zhang, X.Y. Huang, Targeted inhibition of fascin function blocks tumour invasion and metastatic colonization, Nat. Commun. 6 (2015), 7465. https://doi.org/10.1038/ncomms8465.

[13] H.A. Kenny, T. Krausz, S.D. Yamada, E. Lengyel, Use of a novel 3D culture model to elucidate the role of mesothelial cells, fibroblasts and extra-cellular matrices on adhesion and invasion of ovarian cancer cells to the omentum, Int. J. Cancer 121 (2007) 1463–1472, https://doi.org/10.1002/ijc.22874.

[14] P.N. Peters, E.M. Schryver, E. Lengyel, H. Kenny, Modeling the early steps of ovarian cancer dissemination in an organotypic culture of the human peritoneal cavity, J. Vis. Exp. (2015), e53541. https://doi.org/10.3791/53541.

[15] A.K. Mitra, M. Zillhardt, Y.J. Hua, P. Tiwari, A.E. Murmann, M.E. Peter, E. Lengyel, MicroRNAs reprogram normal fibroblasts into cancer-associated fibroblasts in ovarian cancer, Cancer Discov. 2 (2012) 1100–1108, https://doi.org/10.1038/onc.2015.89.

[16] H.A. Kenny, C.Y. Chiang, E.A. White, E.M. Schryver, M. Habis, I.L. Romero, A. Ladanyi, C.V. Penicka, J. George, K. Matlin, A. Montag, K. Wroblewski, S.D. Yamada, A.P. Mazar, D. Bowtell, E. Lengyel, Mesothelial cells promote early ovarian cancer metastasis through fibronectin secretion, J. Clin. Investig. 124 (2014) 4614–4628, https://doi.org/10.1172/JCI74778.

[17] H.A. Kenny, P. Leonhardt, A. Ladanyi, S.D. Yamada, A. Montag, H.K. Im, S. Jagadeeswaran, D.E. Shaw, A.P. Mazar, E. Lengyel, Targeting the urokinase plasminogen activator receptor inhibits ovarian cancer metastasis, Clin. Cancer Res. 17 (2011) 459–471, https://doi.org/10.1158/1078-0432.CCR-10-2258.

[18] M. Curtis, H.A. Kenny, B. Ashcroft, A. Mukherjee, A. Johnson, Y. Zhang, Y. Helou, R. Batle, X. Liu, N. Gutierrez, X. Gao, S.D. Yamada, R. Lastra, A. Montag, N. Ahsan, J.W. Locasale, A.R. Salomon, A.R. Nebreda, E. Lengyel, Fibroblasts mobilize tumor cell glycogen to promote proliferation and metastasis, Cell Metab. (2018)https://doi.org/10.1016/j.cmet.2018.08.007 pii: S1550-4131(18)30508-4 [Epub ahead of print].

[19] H.A. Kenny, E. Lengyel, MMP-2 functions as an early response protein in ovarian cancer metastasis, Cell Cycle 8 (2009) 683–688, https://doi.org/10.4161/cc.8.5.7703.

[20] S. Domcke, R. Sinha, D.A. Levine, C. Sander, N. Schultz, Evaluating cell lines as tumour models by comparison of genomic profiles, Nat. Commun. 4 (2013), 2126. https://doi.org/10.1038/ncomms3126.

[21] S. Han, J. Huang, B. Liu, B. Xing, F. Bordeleau, C.A. Reinhart-King, W. Li, J.J. Zhang, X.Y. Huang, Improving fascin inhibitors to block tumor cell migration and metastasis, Mol. Oncol. 10 (2016) 966–980, https://doi.org/10.1016/j.molonc.2016.03.006.

[22] J. Huang, R. Dey, Y. Wang, J. Jakoncic, I. Kurinov, X.Y. Huang, Structural insights into the induced-fit inhibition of fascin by a small-molecule inhibitor, J. Mol. Biol. 430 (2018) 1324–1335, https://doi.org/10.1016/j.jmb.2018.03.009.

[23] L. Chen, S. Yang, J. Jakoncic, J.J. Zhang, X.Y. Huang, Migrastatin analogues target fascin to block tumour metastasis, Nature 464 (2010) 1062–1066, https://doi.org/10.1038/nature08978.

[24] A.K. Mitra, C.Y. Chiang, P. Tiwari, S. Tomar, K.M. Watters, M.E. Peter, E. Lengyel, Microenvironment-induced downregulation of miR-193b drives ovarian cancer metastasis, Oncogene 34 (2015) 5923–5932, https://doi.org/10.1038/onc.2015.43.

[25] M. Lal-Nag, L. McGee, R. Guha, E. Lengyel, H.A. Kenny, M. Ferrer, A high-throughput screening model of the tumor microenvironment for ovarian cancer cell growth, SLAS Discov. 22 (2017) 494–506, https://doi.org/10.1177/2472555216687082.

[26] A.J. Ridley, Rho GTPase signalling in cell migration, Curr. Opin. Cell Biol. 36 (2015) 103–112, https://doi.org/10.1016/j.ceb.2015.08.005.

[27] H.E. Johnson, S.J. King, S.B. Asokan, J.D. Rotty, J.E. Bear, J.M. Haugh, F-actin bundles direct the initiation and orientation of lamellipodia through adhesion-based signaling, J. Cell Biol. 208 (2015) 443–455, https://doi.org/10.1083/jcb.201406102.

[28] Y. Hashimoto, M. Parsons, J.C. Adams, Dual actin-bundling and protein kinase C-binding activities of fascin regulate carcinoma cell migration downstream of Rac and contribute to metastasis, Mol. Biol. Cell 18 (2007) 4591–4602, https://doi.org/10.1091/mbc.e07-02-0157.

[29] H. Fu, J.-F. Wen, Z.-L. Hu, G.-Q. Luo, H.-Z. Ren, Knockdown of fascin1 expression suppresses the proliferation and metastasis of gastric cancer cells, Pathology 41 (2009) 655–660, https://doi.org/10.3109/00313020903273100.

[30] I.L. Romero, A. Mukherjee, H.A. Kenny, L.M. Litchfield, E. Lengyel, Molecular pathways: trafficking of metabolic resources in the tumor microenvironment, Clin. Cancer Res. 21 (2015) 680–686, https://doi.org/10.1158/1078-0432.CCR-14-2198.

[31] E. Kostopoulou, A. Daponte, A. Terzis, M. Nakou, I. Chiotoglou, D. Theodosiou, C. Chatzichristodoulou, I.E. Messinis, G. Koukoulis, Fascin in ovarian epithelial tumors, Histol. Histopathol. 23 (2008) 935–944, https://doi.org/10.14670/HH-23.935.

[32] I.H. Ozerhan, N. Ersoz, O. Onguru, M. Ozturk, B. Kurt, S. Cetiner, Fascin expression in colorectal carcinomas, Clinics 65 (2010) 157–164, https://doi.org/10.1590/S1807-59322010000200007.

[33] R. Kozma, S. Ahmed, A. Best, L. Lim, The Ras-related protein Cdc42Hs and bradykinin promote formation of peripheral actin microspikes and filopodia in Swiss 3T3 fibroblasts, Mol. Cell. Biol. 15 (1995) 1942–1952.

[34] J.C. Adams, M.A. Schwartz, Stimulation of fascin spikes by thrombospondin-1 is mediated by the Gtpases Rac and Cdc42, J. Cell Biol. 150 (2000) 807–822.